PCCP

Temperature-Dependence of the Dielectric Relaxation of Water using Non-Polarizable Water Models

Journal:	*Physical Chemistry Chemical Physics*
Manuscript ID	CP-ART-08-2019-004578.R1
Article Type:	Paper
Date Submitted by the Author:	15-Nov-2019
Complete List of Authors:	Zarzycki, Piotr; Lawrence Berkeley National Laboratory, Energy Geociences Division Gilbert, Benjamin; Lawrence Berkeley National Laboratory, Energy Geosciences Division

Temperature-Dependence of the Dielectric Relaxation of Water using Non-Polarizable Water Models

Piotr Zarzycki[1] and Benjamin Gilbert[1]

[1] *Energy Geoscience Division, Lawrence Berkeley National Laboratory, Berkeley, CA 94720 USA*

ABSTRACT

Key physical and chemical properties of aqueous fluids are determined by the structure and dynamics of the hydrogen bond network of water but we lack adequate models for the linkages between hydrogen bonding and aqueous chemistry, particularly in non-ambient conditions or in confinement. Dielectric relaxation spectroscopy (DRS) provides a sensitive approach for probing water dynamics but sound interpretation of DRS data requires molecular simulation and associated computational methods capable of accurately representing aqueous fluids and their frequency dependent, complex permittivity. Here, we test the accuracy of dielectric spectra of bulk liquid water calculated from molecular dynamics simulations using 19 non-polarizable water models at 298K. In contrast to prior studies, the simulation size, time-step and duration allow calculation of the dielectric function from 10^7–10^{12} Hz without assuming an analytical form. The accuracy of the prediction of the low-frequency (static) dielectric constant at room temperature is related to the water molecule dipole moment, specifically models with $\mu \geq 2.4$D give $\varepsilon(0)$ with a relative error

lower than 5%. However, no water model tested can fully reproduce the complex dielectric spectra of water. For a subset of models, calculations of the dielectric response from -5–60C reproduces the experimental trend in water dynamics with temperature but the characteristic relaxation time is always under estimated. The calculated water dipole relaxation time and hydrogen-bond lifetime are both exponentially decaying functions of temperature, and exhibit a linear correlation very close to equality. The comparison provides new computational support for the concept that the Debye relaxation of liquid water is determined by the dynamics of the hydrogen-bond network, and that both are ensemble properties.

INTRODUCTION

Aqueous chemical processes are central to all hydrological and (geo)biological cycles that maintain life on the planet[1-3] but descriptions of the molecular structure and chemical properties of aqueous fluids, particularly in non-ambient conditions or in confinement, remain incomplete. Key physical and chemical attributes of aqueous fluids are determined by the hydrogen bond network of dipolar water molecules. For example, the solvation of ions requires hydrogen-bonded water molecules to polarize and reorganize around a solute.[4, 5] However, no individual method is capable of directly elucidating the structure and properries of hydrogen-bond networks. Valuable insights into the hydrogen-bond network of aqueous fluids can be obtained from dielectric relaxation spectroscopy (DRS), which measures the frequency-dependent, complex permittivity $\varepsilon(\omega) = \varepsilon'(\omega) - i\varepsilon''(\omega)$, where $i = \sqrt{-1}$.[6-8] The dielectric response of bulk liquid water is dominated by the Debye relaxation, a large change in the permittivity that occurs in the microwave range ($\nu \in$ 1-300 GHz) with the inflection point in $\varepsilon'(\omega)$ at approximately 19 GHz at room temperature. Hydrophilic and hydrophobic solutes, ion pair formation and other solution interactions can shift relaxation frequency and introduce additional relaxations to a DRS

spectrum.[6-8] In addition, water that is strongly bound to a solute or a surface typically exhibits a dielectric response shifted to lower frequencies.[9] In general, the spectrum is complex, and its deconvolution into responses of individual components and distinct relaxation processes remains a major challenge. [6, 9]

The most informative approach for interpreting DRS data would use molecular simulations that accurately predict the hydrogen-bond dynamics of a system from which DRS spectra could be calculated for comparison with experimental data. Methods for predicting DRS spectra from atomic trajectories in molecular simulations have been developed over decades[10-14] but remain far from routine because the large frequency range of aqueous relaxation phenomena demands both a small time step and a large simulation time. As a consequence, earlier studies were unable to statistically sample the necessary timescales and fitted analytical response functions to the noisy predicted relaxation behaviour. This process introduces ambiguity because debate remains over the most appropriate approach for the decomposition of DRS data from water into one or more contributions. Classical molecular dynamics (MD) simulations can increasingly access large dynamical timescales enabling direct comparison with experiment.

In this study, we evaluate the ability of rigid, static-point-charge models, which are non-polarizable, to reproduce the complex permittivity of bulk liquid water at 298K. For a subset of the best performing models we also report calculations of $\varepsilon(\omega)$ from -5–60C. This work complements recent study by Cardona *et al.*[14, 15] who compared different molecular models for predicting the DRS of water and organic molecules as a prelude to the simulation of microwave heating, and work by Sega and Schröder[13] who compared polarizable and nonpolarizable water molecules for predicting the dielectric and far-infrared spectra.

METHODS

Water Models

The interatomic potentials (force fields) that define the water models used in this study are based on pair-wise non-bonded Lennard-Jones and electrostatic interactions, usually with the Lennard-Jones parameters only assigned to the oxygen atom. The positive partial charges are assigned to the hydrogen atoms, the negative charge is assigned to either the oxygen atom (3-point models), a virtual site located on the HOH angle bisector (4-point models) or virtual sites completing the tetrahedral oxygen-coordination (5-point models). The force fields have been constructed with different levels of complexity and optimized to different sets of physicochemical properties[16-18] that can include: structure (*e.g.*, radial distribution functions), equation of state, self-diffusion coefficient, experimental gas-phase water dipole moment, liquid-phase dipole moment predicted using *an initio* methods, and the static dielectric constant. However, it is currently intractable to consider complex dynamical properties such as dielectric relaxation or heat capacities in force-field development.

We chose the most popular water force-fields (e.g., SPC[19], SPC/E,[20] TIP3P,[21] TIP4P,[21] TIP5P[22]) and a few recently developed models that can reproduce the static dielectric constant of liquid water at 298K (OPC,[23] OPC3,[23] TIP4Q,[24] TIP4P/ε,[22] SPC-DC,[25] H2O-DC,[25] TIP3P-FB,[26] TIP4P-FB[26]). We also analysed the performance of the classical TIP*n*P water models that have been revised for use with the particle-mesh Ewald (PME) method (i.e., TIP3PF,[27] TIP4PEW,[28] TIP5PEW[29]) and include one flexible water model (SPC/FW^{REF}). The parameters used in the water models given in **Table 1.**

The simulations presented here do not consider the nuclear quantum effects that are known to affect the structure and dynamics of the hydrogen-bonding structure in liquid water via tunneling,

proton delocalization, and intermolecular zero-point energy quantum fluctuations.[30-35] The NQE effects are neglected for several reasons. First, the NQE produces the competing quantum effects on the HB network: weakening the weak HB bonds and strengthening the strong ones – overall canceling each other to a large extent in the bulk water at ambient conditions.[33-35] Second, the ab initio path integral molecular dynamics is computationally too expensive to obtain nanosecond-range trajectories required to calculate the dielectric spectra. Finally, the NQE have relatively small effect on the average dipole moment of a water molecule in the bulk.[30, 34]

Table 1. Force field parameters for non-polarizable water models used in our simulations.

Water model		Lennard-Jones parameters		partial charges			Geometry			Dipole moment[c]
		σ_O (Å)	ε_O (kcal/mol)	q_O (e)	μ (D)	$q_{O/x}$ (e)	r_{OH} (Å)	∠HOH (°)	r_{OX} (Å)	μ (D)
three-point models										
SPC	ref.[19]	3.1657	0.1553	-0.8400	0.4200		1.000	109.47		2.274
SPC/E	ref.[20]	3.1657	0.1553	-0.8476	0.4238		1.000	109.47		2.350
SPC/E$_B$	ref.[36]	3.1657	0.1553	-0.8476	0.4238		1.010	109.47		2.374
SPC/FW[a]	ref.[37]	3.1657	0.1554	-0.8200	0.4100		1.012	107.57		2.395
SPC-DC	ref.[25]	3.1577	0.1984	-0.8736	0.4368		1.000	109.47		2.423
TIP3P	ref.[21]	3.1506	0.1520	-0.8340	0.4170		0.957	104.52		2.348
TIP3PF	ref.[27]	3.1941	0.0980	-0.8300	0.4150		0.957	104.52		2.336
TIP3P-FB	ref.[26]	3.1780	0.1559	-0.8484	0.4242		0.957	104.52		2.419
H_2O-DC	ref.[25]	3.1840	0.1417	-0.9099	0.4550		0.958	109.47		2.411
OPC3	ref.[23]	3.1743	0.1634	-0.8952	0.4476		0.979	109.47		2.430
four-point models										
OPC	ref.[23]	3.1666	0.2128	0.0000	0.6791	-1.3583	0.872	103.60	0.159	2.480
TIP4P	ref.[21]	3.1537	0.1550	0.0000	0.5200	-1.0400	0.957	104.52	0.150	2.178
TIP4PEW	ref.[28]	3.1643	0.1628	0.0000	0.5200	-1.0484	0.957	104.52	0.125	2.322
TIP4P-FB	ref.[26]	3.1655	0.1791	0.0000	0.5259	-1.0517	1.012	108.15	0.105	2.429
TIP4P2005	ref.[38]	3.1589	0.1852	0.0000	0.5564	-1.1128	0.957	104.52	0.155	2.304
TIP4Q	ref.[24]	3.1666	0.1852	0.5000	0.5250	-1.5500	0.957	104.52	0.069	2.442
TIP4P/ε	ref.[22]	3.1650	0.1848	0.0000	0.5270	-1.0540	0.957	104.52	0.105	2.435
five-point models										
TIP5P[b]	ref.[22]	3.1199	0.1600	0.0000	0.2410	-0.2410	0.957	104.52	0.700	2.293
TIP5PEW[b]	ref.[29]	3.0970	0.1780	0.0000	0.2410	-0.2410	0.957	104.52	0.700	2.293

[a]flexible water model (HOH angle flexibility modelled with a harmonic function, $k_{\angle HOH}$ =37.95 kcal/mol/rad^2)[37]
[b]two negatively charged virtual sites X with an angle ∠XOX = 109.47°
[c]experimental value 2.4-2.95D,[39, 40] theoretical estimation from the ab-initio molecular dynamics ~3D[41, 42]

Molecular Dynamic Simulation

Dielectric spectra and hydrogen-bond analysis were carried out by analysing classical MD trajectories obtained using *pmemd* simulation engine from the Amber18 package.[43] The initial

atom configurations were minimized using the mixture of the steepest descent and conjugate gradient minimization schemes. Next, the system was brought to the desired temperature by heating or cooling for 100 ps, (NVT ensemble) using Langevin thermostat (collision frequency γ=1.0 ps $^{-1}$). In the next step, we optimize the density and volume of the cell by running molecular dynamics in the isobaric-isothermal ensemble (NPT) for additional 5 ns (Berendsen barostat with the pressure relaxation time τ=2 ps, Langevin thermostat with γ=1.0 ps $^{-1}$). The final simulations were carried out using the optimized cell volume in the NVT ensemble for another 30 ns (Langevin thermostat, γ=1.0 ps $^{-1}$). The value of the collision frequency in the Langevin dynamics affects the rate of convergance of static dielectic constant and controls stochastic variation between simulations starting from the identicial initial state as illustrated in Fig. S3. However, it does not significantly alter the long-time averages, and therefore the simulations are carried out for γ=1.0 ps $^{-1}$. In all simulations we used the integrator time-step of 2 fs. The configurations were saved every 0.2 ps (for calculating dielectric spectra) or 0.05 ps (for HB-analysis). The long-range electrostatic interactions were calculated using the Particle Mesh Ewald summation method (PME). The simulations presented here were obtained for a box of 17000 water molecules (**Fig. 1**) and a short-range interaction cut-off of 16 Å – settings necessary to include the dipole-dipole correlation beyond the second-solvation shell. [44] In addition, simulation of a larger number of water molecules reduces the noise in the autocorrelation function and the calculated $\varepsilon(\nu)$ because the fluctuations in the system properties are proportional to $1/\sqrt{N_{H_2O}}$. The final trajectory was analysed using analysis codes developed in C++ and Python.

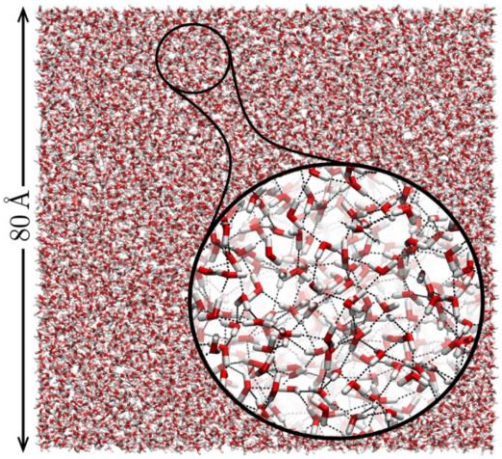

Figure 1 Snapshot of the simulation cell with 17,000 H_2O water molecules. Inset illustrates the hydrogen-bond network in the liquid water.

Dielectric Properties

The water static dielectric constant, $\varepsilon(0)$, is a collective property of an ensemble of water dipoles, which can be calculated from the equilibrium total dipole moment fluctuations, $\langle M^2 \rangle - \langle M \rangle^2$. The static dielectric constant is usually calculated using the following Clausius-Mosotti type equation[44]

$$\varepsilon(0) = 1 + \frac{\langle M^2 \rangle - \langle M \rangle^2}{3\varepsilon_0 V k_B T} \quad (1)$$

where ε_0 is the vacuum permittivity, V is the volume of an aqueous phase and M is the total dipole moment of the ensemble of molecular dipoles ($\vec{M} = \sum_i \vec{\mu}_i$).

The frequency-dependent dielectric constant is obtained from the Fourier-Laplace transform of the time-derivative of the normalized autocorrelation function of the total dipole moment, ϕ: [44]

$$\frac{\varepsilon(\omega)-1}{\varepsilon(0)-1} = \int_0^\infty \left(-\frac{d\phi(t)}{dt}\right) e^{-i\omega t} dt \quad (2)$$

where

$$\phi(t) = \frac{\langle M(t)M(0)\rangle}{M^2} \quad (3)$$

By replacing the Fourier-Laplace transform by a half of the Fourier transform, and using eq. (1) we obtain:

$$\varepsilon(\omega) = 1 + \frac{\langle M^2\rangle - \langle M\rangle^2}{6\varepsilon_0 V k_B T}\int_{-\infty}^{\infty}\left(-\frac{d\phi(t)}{dt}\right)e^{-i\omega t}dt \quad (4)$$

The local ordering and fluctuations of the dipole moments are usually quantified by the finite (G_K) and infinite (g_K) system Kirkwood correlation factors, which are defined as:

$$G_K = \frac{\langle M^2\rangle - \langle M\rangle^2}{N\langle\mu^2\rangle} \quad \text{and} \quad g_K = \frac{2\varepsilon(0)+1}{3\varepsilon_0}G_K \quad (5)$$

The G_K factor measures the equilibrium fluctuations of the collective dipole moment of the system and it is related to the orientational correlation function. The g_k factor measures local the correlation between neighbouring dipole moments, for instance it can indicate the antiparallel ($g_k<1$), random ($g_k=1$) or parallel neighbouring dipoles mutual orientation.

Analytical Debye Relaxation Models

The dominant water dipolar relaxation mode is accurately described by the Debye function:[6-8, 45]

$$\varepsilon(\omega) = \varepsilon_\infty + \frac{\varepsilon(0)-\varepsilon_\infty}{1+i\omega\tau_D} \quad (6)$$

where $\varepsilon_\infty = \lim_{\omega\to\infty}\varepsilon'$ and τ_D is the Debye relaxation time, which is defined as the period of the electromagnetic wave at the frequency of the maximum in ε'' ($\tau_D = \omega_D^{-1} = 1/2\pi\nu_D$). Quantitative determination of τ_D is typically obtained by least-squares fitting but there is disagreement in the literature on the number of relaxation contributions and the choice of a Debye function or a more complex analytical form.[6, 9] Here we used a model-free approach to comparing simulation and experiment and read off τ_D directly from the peak position in the dielectric loss function. For visual

comparisons, the simulated dielectric spectra are plotted against experimental data from the literature,[2, 3] and their fit to a single Debye function.

Hydrogen-Bond Lifetime

Of the many definitions of the hydrogen-bond lifetime[46], here we followed Luzar and Chandler and use a reactive flux approach.[47, 48] The interrupted hydrogen-bond lifetime is calculated from the time derivative of the hydrogen-bond correlation function, $c(t)$, given by an average over the simulation ensemble:[46-48]

$$c(t) = \frac{\langle h(0)h(t)\rangle}{\langle h^2\rangle} \quad (8)$$

where h(t) is a binary classification function associated with each pair of water molecules: $h = 1$ if a given pair is hydrogen bonded, and $h = 0$ otherwise. Thus, $c(t)$ measures the probability that two water molecules remain hydrogen-bonded at the time t if they were bonded at the time $t = 0$.[46] Two water molecules are considered to be hydrogen-bonded if oxygen-oxygen distance (r_{OO}) is not larger than 3.5 Å and hydrogen-donor-acceptor angle below $30°$.[48]

The reactive flux rate, $K(t)$, for hydrogen-bond breaking is defined as a difference between the rate of HB-breaking (k_b) and HB-(re)forming (k_f):.[46-48]

$$K(t) = -\frac{dc(t)}{dt} = k_b c(t) - k_f n(t) \quad (7)$$

where k_f, k_b are rate constants for HB (re)forming and breaking, respectively and $c(t)$ as defined above serves as an effective source term for the HB-bonded molecules. The HB (re)forming rate constant k_f is calculated from the detailed balance condition, that is:[46] $k_f = k_b\langle h\rangle/(1 - \langle h\rangle)$. $n(t)$ gives the probability of breaking an existing hydrogen-bond while two water molecules remain within the HB-bond distance and represents a HB sink in eq. (7):[46, 48]

$$n(t) = \int_0^t -\frac{\langle \frac{dh(0)}{d\xi}\big|_0 (1-h(\xi))H(\xi)\rangle}{\langle h^2\rangle} d\xi \quad (9)$$

where $H(\xi)$ is 1 if water molecules are within the HB-contact distance ($r_{OO} \leq 3.5$ Å), or 0 otherwise.

The hydrogen-bond relaxation time is defined as an inverse of the HB-breaking rate constant (i.e., $\tau_{HB} = k_b^{-1}$).[46] By knowing τ_{HB}, we can estimate the activation barrier for the breaking of the hydrogen-bond. A procedure introduced by Luzar et al.[46-48] assumes that the HB breaking is a thermally activated process (i.e., obeys the Eyring-Polanyi equation):

$$k_b = \frac{1}{\tau_{HB}} = \frac{k_B T}{h} \exp\left(-\frac{\Delta G_{HB}}{k_B T}\right) \quad (10)$$

where h is the Planck's constant, and ΔG_{HB} is the activation barrier ΔG_{HB}, which is an energetic measure of the strength of the HB. It can be calculated from τ_{HB} as follows: [49]

$$\Delta G_{HB} = k_B T \ln\left(\frac{k_B T}{h} \tau_{HB}\right) \quad (11)$$

As noticed by Van Der Spoel et al.,[49] HB-lifetime values obtained using eq. (7) are sensitive to the time-separation between subsequent configurations (Δt). Specifically, τ_{HB} decreases and k_f increases rapidly with the decreasing Δt. [49] The results presented here are obtained consistently for the same Δt values for each water model (i.e., Δt= 50 fs).

RESULTS AND DISCUSSION

The calculated dielectric and hydrogen-bond network properties are given in **Table 2** and compared with the experimental data[2] for water at 298 K. A comparison of the errors in predicted static and dynamic dielectric properties is given in **Figure 2**.

Table 2 Experimental and calculated dielectric properties of water at 298K for 19 nonpolarizable water models. The dielectric properties were obtained by analysing 30 ns molecular dynamics trajectories. The static dielectric constant (ε(0)) is a slowly converging property (see Fig. S1, Supporting Information), the results presented here are within 2% relative error, which usually translates to ±1-2 ε(0) units.

	Permittivity		Debye relaxation		HB-dynamics
Water model	ε(0)	ε(∞)	τ_D (ps)	ν_D (GHz)	τ_{HB} (ps)
SPC	66.61	7.91	**4.72**	33.73	**6.00**
SPC/E	70.80	7.49	**5.66**	28.10	**6.89**
SPC/E$_B$	71.78	7.03	**7.46**	21.33	**8.74**
SPC/FW	83.17	7.95	**6.68**	23.83	**7.417**
SPC-DC	81.08	9.11	**4.99**	31.90	**6.306**
TIP3P	100.9	12.2	**3.42**	46.50	**3.658**
TIP3PF	91.23	9.06	**4.87**	32.67	**4.959**
TIP3P-FB	80.24	7.51	**7.23**	22.00	**7.670**
H_2O-DC	79.37	8.08	**6.27**	25.37	**7.340**
OPC3	80.08	7.98	**5.99**	26.57	**7.539**
OPC	79.50	8.76	**5.70**	27.90	**7.354**
TIP4P	51.56	8.34	**3.33**	47.83	**5.353**
TIP4PEW	64.61	7.65	**5.43**	29.33	**7.160**
TIP4P-FB	76.86	6.59	**6.20**	25.67	**8.493**
TIP4P2005	57.67	7.06	**5.46**	29.13	**7.966**
TIP4Q	80.87	7.91	**6.77**	23.50	**7.630**
TIP4P/ε	79.18	7.71	**6.76**	23.53	**7.986**
TIP5P	92.44	7.71	**7.16**	22.23	**6.490**
TIP5PEW	98.36	8.04	**6.64**	23.97	**6.173**
Experiment[2, 3]	78.36	5.2	**8.27**	19.24	

Static Dielectric Constant

An assessment of the uncertainty in the predicted values of the static dielectric constant is required for assessing the results from the different models because $\varepsilon(0)$ is a slowly converging property of molecular simulations. Fennell et al.[25] showed that a trajectory of at least 10 ns is needed to converge on $\varepsilon(0)$. However, $\varepsilon(0)$-estimation is also sensitive to molecular dynamics details: molecular dynamics integrator, force-calculation scheme, and the temperature control. For one water model (TIP4P-FB) we examined the convergence of static dielectric properties $(\varepsilon(0), g_K, G_K)$ for simulations that started from the same initial configuration and diverged in time due to the randomness introduced by the Langevin thermostat (g_K, G_K in Table S1). The simulation results obtained from 30-ns trajectories show at least 2-3% variability (**Figs. S1-S2**), which could explain why reported values of $\varepsilon(0)$ for various water models vary between different simulation

studies (e.g., [24, 27, 50]). Among all 19 considered water models we can identify 9 that predict the static dielectric constant of water at room temperature that is within 5% of the experimental value. The remaining 10 water models are unable to correctly predict the static dielectric constant, usually because these models have been developed to reproduce other water properties. Cardona *et al.*[14] proposed scaling $\varepsilon(\omega)$ to the experimentally measured value of $\varepsilon(0)$, but that approach is not adopted here.

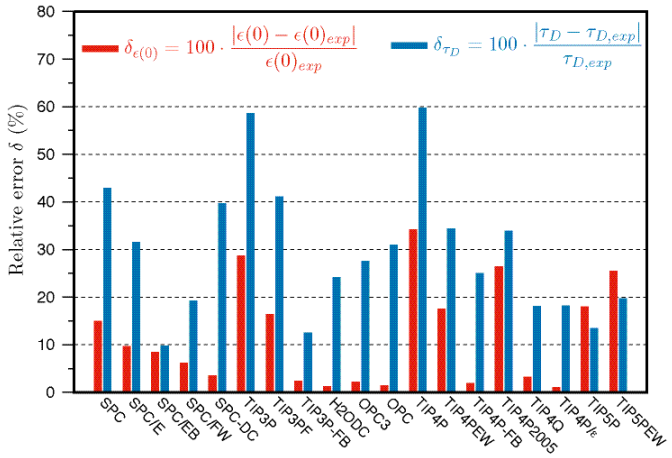

Figure 2. Relative error in predicted static dielectric constant, $\varepsilon(0)$, and Debye relaxation time, τ_D, at room temperature among considered water models (30 ns simulations). The experimental data, $\varepsilon(0)_{exp}, \tau_{D,exp}$, are taken from ref.[3]

Dielectric Relaxation Spectra

The predicted DRS for the 9 water models that provided the best predictions of the static dielectric constant are shown in **Figure 3a**; the dielectric spectra for the remaining models are shown in **Figure 3b**. The comparison shows that accuracy in the prediction in the static dielectric constant is highly correlated with accuracy in representing the frequency-dependent dielectric relaxation. However, none of the water models exactly reproduces the dielectric spectra, as previously observed[13]. For all models, the predicted Debye relaxation time is shorter than the experimental value (τ_D = 8.27 ps; ν_D = 19.24 GHz). Only the 5-point models are able to reproduce

the low-frequency side of the dielectric loss peak at 298 K (see **Fig. 3a,b**), but they still overestimate the values of $\varepsilon(0)$. Although OCP and OCP3 were intended to improve ions and proteins solvation, these models are not optimum for the frequency-dependent dielectric relaxation. TIP3P-FB seems to be the best for both static and dynamic dielectric properties, a likely consequence of the well designed and efficient optimization strategy developed in the force-balance method.[26]

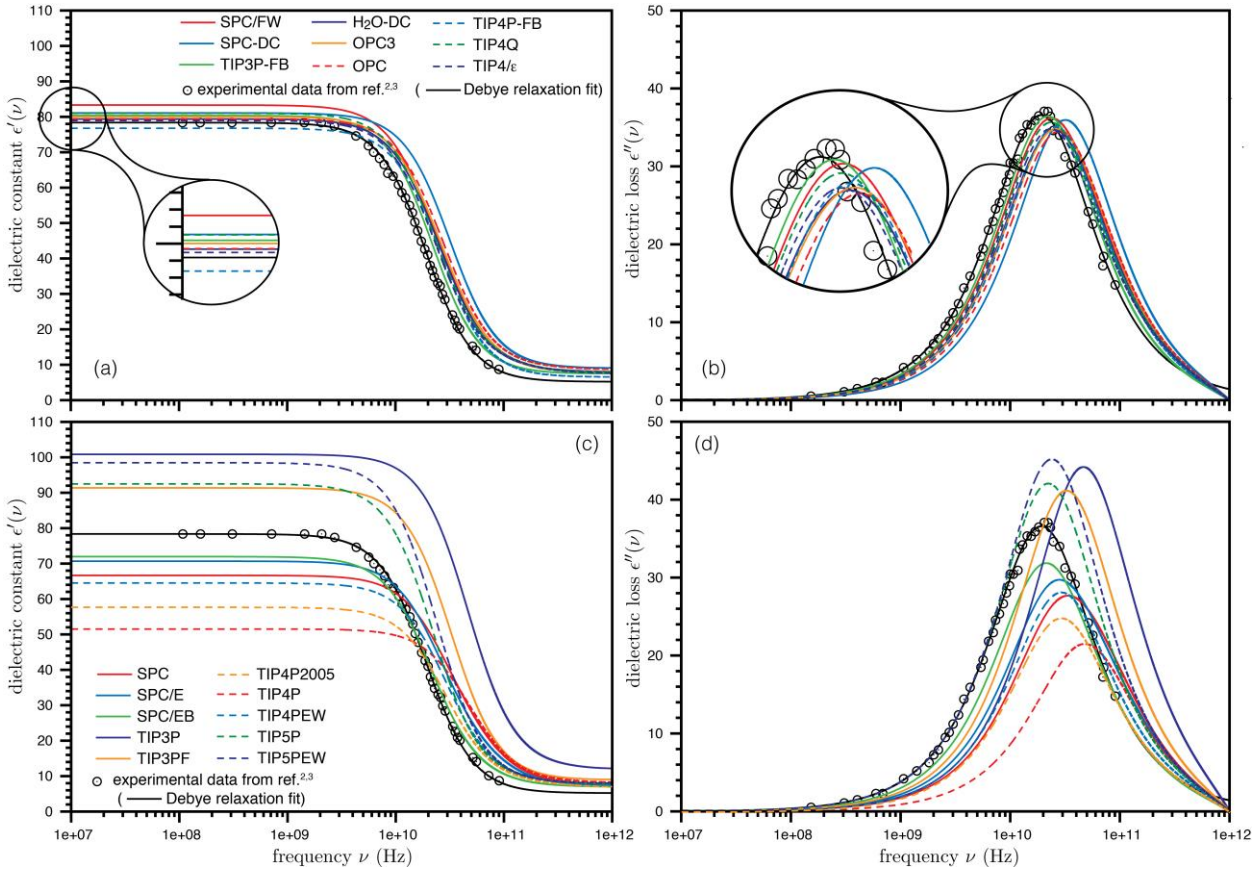

Figure 3. a) Predicted dielectric relaxation spectra of bulk liquid water using 9 water models that gave the smallest relative error in predicted static dielectric constant at 298 K. b) Simulated dielectric spectra using 10 water models with the largest relative error in predicted static dielectric constant at 298 K.

Water Dipole Moment

We find that the relative error in $\varepsilon(0)$ at 298 K obtained for all water models with the dipole moment $\mu > 2.4$ is below 5%. Accordingly, we asked whether a modification to the force-field

parameters to obtain $\mu > 2.4$ would improve the predictions of the dielectric properties. For the TIP5P water model, changing the partial charge from 0.241 to 0.2555 ($q_H = -q_x$) achieves $\mu =$ 2.43 D. The predicted static dielectric constant at 298K is 77.2, a significant improvement over the original prediction of 92.44. However, prediction of the Debye relaxation is severely worsened with τ_D=281 ps, almost two orders of magnitude too slow. This suggests that force-field parametrization of rigid water models must consider the Debye relaxation in order to more accurately capture the dynamical properties of aqueous solutions. Even models that reproduce the self-diffusion coefficient, which captures an aspect of water HB dynamics, do not provide accurate DRS prediction.

Temperature Dependence

We tested the ability of 8 of the 9 best performing models (omitting the flexible model) to reproduce the frequency dependent dielectric spectra of liquid water at temperatures between -5–60˚C (**Figs. S4-S7**) with the results for TIP4P-FB illustrated in **Figure 4**. For these models and this temperature range, the dipolar relaxation consistently occurs at higher frequency (shorter relaxation time) than the experimental data but the discrepancies between the experimental data and predictions for both $\varepsilon(0)$ and $\varepsilon(\nu)$ are approximately constant. Thus, although the models over predict the rotational mobility of water they provide a reasonable prediction of the activation barrier for water reorganization.

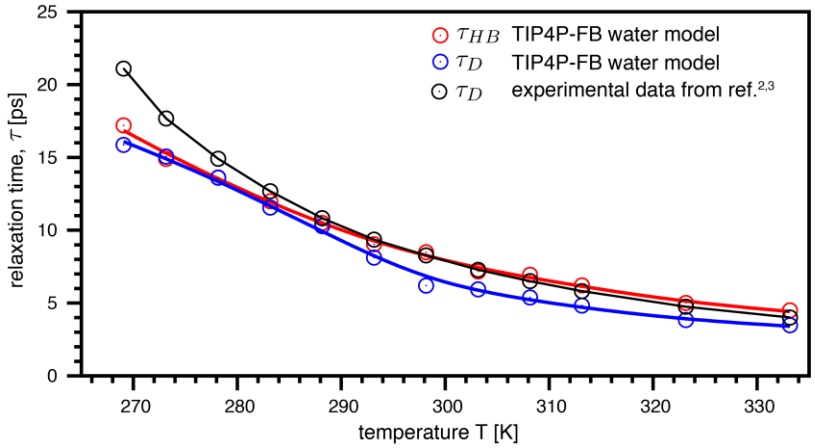

Figure 4 Temperature dependence of the predicted Debye relaxation time, τ_{D}, and hydrogen-bond lifetime, τ_{HB}, for the water TIP4P-FB model, compared with the experimental value of τ_{D} from refs.[2, 3]

The temperature series also highlight that the MD simulations do not accurately reproduce the dissipation of energy caused by water dipole reorientation at frequencies close to the Debye relaxation. The energy loss to the liquid by dielectric relaxation (called dielectric heating) is quantitatively related to the integrated area of $\varepsilon''(\nu)$ (**Figs. S4-S7**). Only the TIP3P-FB closely approximates the dielectric loss function at 269 K (**Fig. S7b**).

Hydrogen Bond Lifetime

By analysing the Debye-relaxation times and hydrogen-bond lifetimes for the temperature series we find that both quantities have a similar in magnitude and have a similar temperature-dependence (illustrated for TIP4P-FB in **Fig. 4**). Plots of τ_D vs τ_{HB} show a robust linear correlation between these properties (**Fig. 5**). The constant of proportionality ranges from 0.92–1.21 and the constant offset ranges between 0.04–2.4 ps. For the best-performing model (TIP4P-FB), the relationship is the closest to equality.

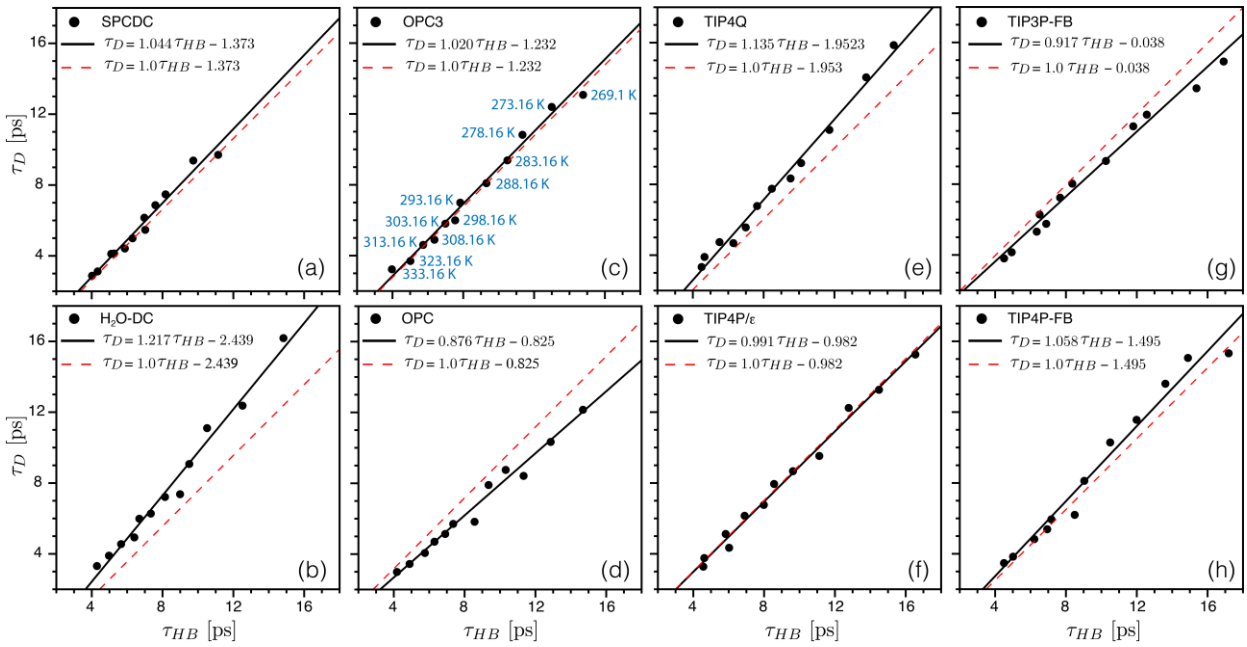

Figure 5. Correlation plots of the Debye relaxation time (τ_D) and the hydrogen-bond lifetime (τ_{HB}) for several water models for the temperature range -5–60˚C. Black points are predictions from individual simulations and black lines are a linear regression of the form $\tau_D(T) = a\tau_{HB}(T) + b$, where T is temperature and a and b are fitted constants displayed for each plot. Red dashed lines are regressions with $a = 1$. The temperature value corresponding to each point is shown in Panel (c) and the points follow the same order in other panels.

CONCLUSION

This work demonstrates that classical molecular dynamics simulation of the dielectric relaxation of water remains challenging and is very sensitive to the force-field parameter values, in agreement with recent studies[13-15] and as previously demonstrated for the static dielectric constant.[24, 27, 50] Even the water models that provide the most accurate predictions of $\varepsilon(0)$ fail to reproduce absolute values for $\varepsilon(\omega)$ including the principal relaxation frequency and the width and amplitude of the dielectric loss peak. Because the dielectric loss peak describes how water dipole reorganization is coupled to energy dissipation and heating, absolute errors in the simulation of aqueous fluids will affect predictions of important properties (heat capacity), physical phenomena (microwave heating) and any chemical phenomena involving entropy changes (*e.g.*, solvation and charge-

transfer processes involving solvent reorganization). Despite these limitations, the best water models predicted dielectric behaviour with consistent accuracy over an important temperature range for geologic, biologic and technologic systems.

Analysis of the temperature-dependent data revealed a close relationship between the mean hydrogen-bond lifetime, calculated for simulation ensembles using the reactive flux method, and the Debye relaxation frequency, also an ensemble property. This finding provides new support for the concept that dipolar relaxation in liquid water is governed by the collective dynamics of the hydrogen-bond network. Although current models of Debye relaxation are based on this intituive assumption,[51-56] it has been challenging to provide full support either from experiment or simulation. Analysis of individual simulation trajectories led to the development of the *wait and switch* model[51-56] in which defects in HB-network are necessary for water molecule to orient in the electric field, but the detailed mechanism, such as the role for hydrogen bond defects, remains debated. Time-resolved two-dimensional infrared (2D IR) spectroscopy experiments determined that hydrogen bond rearrangement requires a collective neighbor response that is likely larger than accessible through trajectory analysis.[57] The present work demonstrates that hydrogen-bond breaking and Debye relaxation are system behaviors with a tight temporal correlation.

Acknowledgements

This work was supported by funding from U.S. Department of Energy (DOE) Chemical Sciences, Geosciences, and Biosciences Division under Contract DE-AC02-05CH11231.

References

1. B. Bagchi, *Water in Biological and Chemical Processes*, Cambridge University Press, Cambridge, 2013.
2. U. Kaatze, *J Chem Eng Data*, 1989, **34**, 371-374.
3. U. Kaatze, *Meas Sci Technol*, 2007, **18**, 967-976.
4. J. D. Smith, R. J. Saykally and P. L. Geissler, *Journal of the American Chemical Society*, 2007, **129**, 13847-13856.
5. P. N. Perera, B. Browder and D. Ben-Amotz, *The Journal of Physical Chemistry B*, 2009, **113**, 1805-1809.
6. F. Kremer and A. Schönhals, *Broadband Dielectric Spectroscopy*, Springer, Berlin, 2003.
7. V. Raicu and Y. Feldman, *Dielectric Relaxation in Biological Systems*, Oxford University Press, Oxford, 2015.
8. R. Pethig, *Dielectrophoresis. Theory, Methodology and Biological Applications*, Wiley, Hoboken, 2017.
9. R. Buchner and G. Hefter, *Phys Chem Chem Phys*, 2009, **11**, 8984-8999.
10. J. Barker and R. Watts, *Molecular Physics*, 1973, **26**, 789-792.
11. M. Neumann, *The Journal of chemical physics*, 1986, **85**, 1567-1580.
12. C. Ro/nne, L. Thrane, P.-O. Åstrand, A. Wallqvist, K. V. Mikkelsen and S. r. R. Keiding, *The Journal of chemical physics*, 1997, **107**, 5319-5331.
13. M. Sega and C. Schroder, *J Phys Chem A*, 2015, **119**, 1539-1547.
14. J. Cardona, M. B. Sweatman and L. Lue, *The Journal of Physical Chemistry B*, 2018, **122**, 1505-1515.
15. J. Cardona, R. Fartaria, M. B. Sweatman and L. Lue, *Molecular Simulation*, 2016, **42**, 370-390.
16. B. Guillot, *J Mol Liq*, 2002, **101**, 219-260.
17. I. Shvab and R. J. Sadus, *Fluid Phase Equilibr*, 2016, **407**, 7-30.
18. C. Vega and J. L. F. Abascal, *Phys Chem Chem Phys*, 2011, **13**, 19663-19688.
19. H. J. C. Berendsen, J. P. M. Postma, W. F. Van Gunsteren and J. Hermans, in *Intermolecular Forces*, ed. B. Pullman, Springer, Dordrecht, 1981, pp. 331–343.
20. H. J. C. Berendsen, J. R. Grigera and T. P. Straatsma, *J Phys Chem-Us*, 1987, **91**, 6269-6271.
21. W. L. Jorgensen, J. Chandrasekhar, J. D. Madura, R. W. Impey and M. L. Klein, *J Chem Phys*, 1983, **79**, 926-935.
22. R. Fuentes-Azcatl and J. Alejandre, *J Phys Chem B*, 2014, **118**, 1263-1272.
23. S. Izadi, R. Anandakrishnan and A. V. Onufriev, *J Phys Chem Lett*, 2014, **5**, 3863-3871.
24. J. Alejandre, G. A. Chapela, H. Saint-Martin and N. Mendoza, *Phys Chem Chem Phys*, 2011, **13**, 19728-19740.
25. C. J. Fennell, L. B. Li and K. A. Dill, *J Phys Chem B*, 2012, **116**, 6936-6944.
26. L. P. Wang, T. J. Martinez and V. S. Pande, *J Phys Chem Lett*, 2014, **5**, 1885-1891.
27. D. J. Price and C. L. Brooks, *J Chem Phys*, 2004, **121**, 10096-10103.
28. H. W. Horn, W. C. Swope, J. W. Pitera, J. D. Madura, T. J. Dick, G. L. Hura and T. Head-Gordon, *J Chem Phys*, 2004, **120**, 9665-9678.
29. S. W. Rick, *J Chem Phys*, 2004, **120**, 6085-6093.
30. M. Ceriotti, W. Fang, P. G. Kusalik, R. H. McKenzie, A. Michaelides, M. A. Morales and T. E. Markland, *Chem Rev*, 2016, **116**, 7529-7550.

31. F. Paesani, S. Yoo, H. J. Bakker and S. S. Xantheas, *J Phys Chem Lett*, 2010, **1**, 2316-2321.
32. M. Ceriotti, J. Cuny, M. Parrinello and D. E. Manolopoulos, *P Natl Acad Sci USA*, 2013, **110**, 15591-15596.
33. S. Habershon, T. E. Markland and D. E. Manolopoulos, *J Chem Phys*, 2009, **131**.
34. X. Z. Li, B. Walker and A. Michaelides, *P Natl Acad Sci USA*, 2011, **108**, 6369-6373.
35. J. A. Morrone and R. Car, *Phys Rev Lett*, 2008, **101**.
36. K. Takemura and A. Kitao, *J Phys Chem B*, 2012, **116**, 6279-6287.
37. Y. J. Wu, H. L. Tepper and G. A. Voth, *J Chem Phys*, 2006, **124**, 024503/024501-024512.
38. J. L. F. Abascal and C. Vega, *J Chem Phys*, 2005, **123**.
39. J. K. Gregory, D. C. Clary, K. Liu, M. G. Brown and R. J. Saykally, *Science*, 1997, **275**, 814-817.
40. Y. S. Badyal, M. L. Saboungi, D. L. Price, S. D. Shastri, D. R. Haeffner and A. K. Soper, *J Chem Phys*, 2000, **112**, 9206-9208.
41. P. L. Silvestrelli and M. Parrinello, *Phys Rev Lett*, 1999, **82**, 3308-3311.
42. A. V. Gubskaya and P. G. Kusalik, *J Chem Phys*, 2002, **117**, 5290-5302.
43. D. A. Case, S. R. Brozell, D. S. Cerutti, T. E. Cheatham, V. W. D. Cruzeiro, T. A. Darden, R. E. Duke, D. Ghoreishi, H. Gohlke, A. W. Goetz, D. Greene, R. Harris, N. Homeyer, S. Izadi, A. Kovalenko, T. S. Lee, S. LeGrand, L. B. Li, C. Lin, J. Liu, T. Luchko, R. Luo, D. J. Mermelstein, K. M. Merz, Y. Miao, G. Monard, H. Nguyen, I. Omelyan, A. Onufriev, F. Pan, R. Qi, D. R. Roe, A. Roitberg, C. Sagui, S. Schott-Verdugo, J. Shen, C. L. Simmerling, J. Smith, J. Swails, R. C. Walker, J. Wang, H. Wei, R. M. Wolf, X. Wu, L. Xiao, D. M. York and P. A. Kollman, *Journal*, 2018.
44. D. van der Spoel, P. J. van Maaren and H. J. C. Berendsen, *J Chem Phys*, 1998, **108**, 10220-10230.
45. P. Debye, *Polar Molecules*, The Chemical Catalog Company, New York, 1929.
46. A. Luzar, *J Chem Phys*, 2000, **113**, 10663-10675.
47. A. Luzar and D. Chandler, *Nature*, 1996, **379**, 55-57.
48. A. Luzar and D. Chandler, *J Chem Phys*, 1993, **98**, 8160-8173.
49. D. van der Spoel, P. J. van Maaren, P. Larsson and N. Timneanu, *J Phys Chem B*, 2006, **110**, 4393-4398.
50. P. Hochtl, S. Boresch, W. Bitomsky and O. Steinhauser, *J Chem Phys*, 1998, **109**, 4927-4937.
51. F. X. Hassion and R. H. Cole, *J Chem Phys*, 1955, **23**, 1756-1761.
52. M. W. Sagal, *J Chem Phys*, 1962, **36**, 2437-+.
53. F. Sciortino, A. Geiger and H. E. Stanley, *Nature*, 1991, **354**, 218-221.
54. S. Schwerdtfeger, F. Kohler, R. Pottel and U. Kaatze, *J Chem Phys*, 2001, **115**, 4186-4194.
55. U. Kaatze, R. Behrends and R. Pottel, *J Non-Cryst Solids*, 2002, **305**, 19-28.
56. T. Sato and R. Buchner, *J Chem Phys*, 2003, **118**, 4606-4613.
57. R. A. Nicodemus, S. Corcelli, J. Skinner and A. Tokmakoff, *The Journal of Physical Chemistry B*, 2011, **115**, 5604-5616.